

AD-A172 339

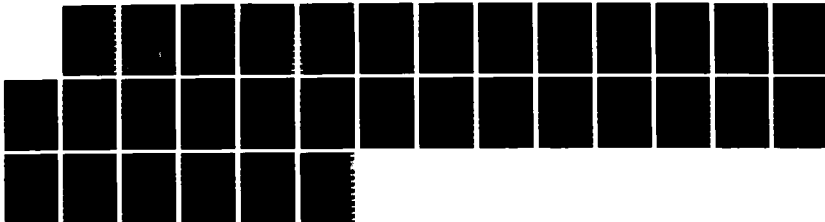
NMR DCS TMA AND HIGH PRESSURE ELECTRICAL CONDUCTIVITY  
STUDIES IN SOLID CR. (U) NAVAL ACADEMY ANNAPOLIS MD  
DEPT OF PHYSICS J J FONTANELLA ET AL. 01 SEP 86 TR-25  
N00014-86-F-00001

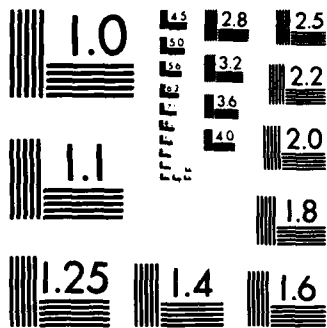
1/1

UNCLASSIFIED

F/G 7/4

NL





1057

12

AD-A172 339

OFFICE OF NAVAL RESEARCH  
Contract N00014-86-AF-00001  
R&T Code 413d001---01  
Technical Report No. 25

NMR, DSC, TMA, and High Pressure Electrical Conductivity Studies in  
Solid, Crosslinked Dimethylsiloxane-ethylene oxide Copolymer Networks  
Containing Sodium

by

John J. Fontanella & Mary C. Wintersgill

Prepared for Publication

in

Polymer

U. S. Naval Academy  
Department of Physics  
Annapolis, MD 21402

September 1, 1986

SDTIC  
ELECTE  
SEP 29 1986  
E

DTIC FILE COPY

Reproduction in whole or in part is permitted for any  
purpose of the United States Government

This document has been approved for public release  
and sale; its distribution is unlimited

86 9 29 097

AD-A172339

Unclassified  
SECURITY CLASSIFICATION OF THIS PAGE

REPORT DOCUMENTATION PAGE

1a. REPORT SECURITY CLASSIFICATION Unclassified		1b. RESTRICTIVE MARKINGS	
2a. SECURITY CLASSIFICATION AUTHORITY		3. DISTRIBUTION / AVAILABILITY OF REPORT This document has been approved for public release and sale; its distribution is unlimited.	
2b. DECLASSIFICATION / DOWNGRADING SCHEDULE		4. PERFORMING ORGANIZATION REPORT NUMBER(S) 25	
4. PERFORMING ORGANIZATION REPORT NUMBER(S) 25		5. MONITORING ORGANIZATION REPORT NUMBER(S)	
6a. NAME OF PERFORMING ORGANIZATION U. S. Naval Academy	6b. OFFICE SYMBOL (if applicable)	7a. NAME OF MONITORING ORGANIZATION Office of Naval Research	
6c. ADDRESS (City, State, and ZIP Code) Physics Department Annapolis, MD 21402-5026		7b. ADDRESS (City, State, and ZIP Code) 800 N. Quincy St. Arlington, VA 22217-5000	
8a. NAME OF FUNDING / SPONSORING ORGANIZATION Office of Naval Research	8b. OFFICE SYMBOL (if applicable)	9. PROCUREMENT INSTRUMENT IDENTIFICATION NUMBER	
8c. ADDRESS (City, State, and ZIP Code) 800 N. Quincy Street Arlington, VA 22217-5000		10. SOURCE OF FUNDING NUMBERS	
		PROGRAM ELEMENT NO. 61153N	PROJECT NO. RR013-06-0C
		TASK NO. 627-793	WORK UNIT ACCESSION NO.
11. TITLE (Include Security Classification) NMR, DSC, TMA, and High Pressure Electrical Conductivity Studies in Solid, Crosslinked Dimethylsiloxane-ethylene oxide copolymer networks Containing Sodium (Unclassified)			
12. PERSONAL AUTHOR(S) John J. Fontanella and Mary C. Wintersgill			
13a. TYPE OF REPORT Interim	13b. TIME COVERED FROM _____ TO _____	14. DATE OF REPORT (Year, Month, Day) 1986 September 1	15. PAGE COUNT 31
16. SUPPLEMENTARY NOTATION			
17. COSATI CODES		18. SUBJECT TERMS (Continue on reverse if necessary and identify by block number)	
FIELD	GROUP	SUB-GROUP	
		Solid electrolytes, Polymer electrolytes, Conductivity dimethylsiloxane-ethylene oxide copolymer, NMR	
19. ABSTRACT (Continue on reverse if necessary and identify by block number)			
<p>Audio frequency electrical conductivity and <sup>23</sup>Na NMR studies have been carried out on solid, crosslinked dimethylsiloxane-ethylene oxide copolymer networks containing sodium. The electrical measurements have been carried out in vacuum over the temperature range 5-380K and at pressures up to 0.65 GPa over the temperature range 230-380K. The electrical conductivity exhibits VTF or WLF behavior. From a VTF analysis, E<sub>a</sub> is found to be about 0.11 eV and T<sub>0</sub> is found to be about 45°C below the "central" glass transition temperature as determined by both DSC and TMA. Also, T<sub>0</sub> is found to increase about 50 K/GPa and E<sub>a</sub> increases significantly with pressure. In addition, the high pressure studies show that the activation volume associated with the electrical conductivity decreases from 44 to 23 cm<sup>3</sup>/mol over the temperature range.</p>			
20. DISTRIBUTION / AVAILABILITY OF ABSTRACT <input checked="" type="checkbox"/> UNCLASSIFIED/UNLIMITED <input type="checkbox"/> SAME AS RPT <input type="checkbox"/> DTIC USERS		21. ABSTRACT SECURITY CLASSIFICATION Unclassified	
22a. NAME OF RESPONSIBLE INDIVIDUAL John J. Fontanella		22b. TELEPHONE (Include Area Code) 301-267-3487	22c. OFFICE SYMBOL

19. ABSTRACT (cont'd)

262-323K. The  $^{23}\text{Na}$  NMR measurements reveal the presence of both bound and mobile sodium species, the relative concentrations of which change by about a factor of 10 over the temperature range  $-100$  to  $+100^\circ\text{C}$ . Broadening of the bound  $^{23}\text{Na}$  line above room temperature suggests the possible presence of ion pairs or higher aggregates in the complex.

Keywords: Solid electrolytes; Polymer electrolyte.

Accession For	
NTIS GRA&I	<input checked="" type="checkbox"/>
DTIC TAB	<input type="checkbox"/>
Unannounced	<input type="checkbox"/>
Justification	
By _____	
Distribution/ _____	
Availability Codes	
Avail and/or	
Dist	Special
A-1	



NMR, DSC, TMA, AND HIGH PRESSURE ELECTRICAL CONDUCTIVITY STUDIES IN SOLID,  
CROSSLINKED DIMETHYLSILOXANE-ETHYLENE OXIDE COPOLYMER NETWORKS CONTAINING  
SODIUM\*

M. C. Wintersgill, J. J. Fontanella, M. K. Smith

Physics Department

U. S. Naval Academy

Annapolis, MD 21402

and

S. G. Greenbaum, K. J. Adamic

Physics Department

Hunter College of CUNY

New York, NY 10021

and

C. G. Andeen

Physics Department

Case Western Reserve University

Cleveland, OH 44106

## ABSTRACT

Audio frequency electrical conductivity and  $^{23}\text{Na}$  NMR studies have been carried out on solid, crosslinked dimethylsiloxane-ethylene oxide copolymer networks containing sodium. The electrical measurements have been carried out in vacuum over the temperature range 5-380K and at pressures up to 0.65 GPa over the temperature range 230-380K. The electrical conductivity exhibits VTF or WLF behavior. From a VTF analysis,  $E_a$  is found to be about 0.11 eV and  $T_0$  is found to be about 45°C below the "central" glass transition temperature as determined by both DSC and TMA. Also,  $T_0$  is found to increase about 50 K/GPa and  $E_a$  increases significantly with pressure. In addition, the high pressure studies show that the activation volume associated with the electrical conductivity decreases from 44 to 23  $\text{cm}^3/\text{mol}$  over the temperature range 262-323K. The  $^{23}\text{Na}$  NMR measurements reveal the presence of both bound and mobile sodium species, the relative concentrations of which change by about a factor of 10 over the temperature range -100 to +100°C. Broadening of the bound  $^{23}\text{Na}$  line above room temperature suggests the possible presence of ion pairs or higher aggregates in the complex.

## INTRODUCTION

Poly(dimethylsiloxane-ethylene oxide) (PDMS-EO) copolymers complexed with alkali metal salts have been receiving attention as solid electrolytes.<sup>1-5</sup> The primary reason, of course, is that in general siloxanes have very low glass transition temperatures and this feature is known to enhance ionic conductivity. In a recent paper,<sup>5</sup> several of the authors have reported the synthesis of a highly crosslinked (PDMS-EO) network containing sodium. In addition, various studies, including differential scanning calorimetry (DSC), <sup>23</sup>Na nuclear magnetic resonance (NMR), and vacuum electrical conductivity were presented. It was shown that the room temperature electrical conductivity was relatively large and that the complex had the advantages of being highly amorphous and stable. Consequently, the material is of interest as a potential solid electrolyte.

In the present paper, results for a differently prepared material are reported. In addition, new types of measurements have been carried out including thermomechanical analysis (TMA) and high pressure electrical conductivity.

## EXPERIMENTAL

Preparation of a crosslinked P(DMS-EO):NaCF<sub>3</sub>COO complex has been described in detail elsewhere.<sup>5</sup> In the present study the composition was slightly altered by adding approximately 33% PDMS to the P(DMS-EO) copolymer while keeping the EO/Na ratio fixed at approximately 8:1. This did not appear to improve the conductivity significantly, although the modified material did exhibit better mechanical flexibility. In addition, differences were noted in some of the thermal properties and NMR linewidths as discussed later.

The <sup>23</sup>Na NMR measurements were performed at 81 MHz utilizing standard pulse techniques. Fourier transform spectra were recorded following accumulation of 1000 free induction decays (FID's). Linewidths and relative intensities of the two resolvable lineshape components were extracted from the FID's by selective saturation and subtraction as discussed below.

Audio frequency complex impedance/electrical relaxation measurements have been carried out using a fully automated spectrometer. The key element in the measurements is a CGA-82 microprocessor-controlled bridge operating at seventeen frequencies from 10-10<sup>5</sup> Hz. Vacuum measurements were carried out in a Precision Cryogenics CT-14 dewar controlled by a Lake Shore Cryotronics DRC-82 temperature controller using a silicon diode sensor. The high pressure measurements were carried out in a pressure vessel using Fluorinert (3M Co.) FC-77 electronic liquid as the high pressure fluid. For the electrical measurements, gold electrodes were vacuum evaporated onto the surfaces of the material in either a three-terminal or two-terminal configuration. The samples were about 1 mm

thick and the electrodes about 4 mm in diameter. DSC and TMA measurements were carried out using a computer-controlled DuPont 990 console coupled with a 910 DSC and 943 TMA.

## RESULTS

### Thermal Analysis

Typical penetration TMA results for PDMS-EO complexed with sodium trifluoroacetate are shown in Figure 1. The primary feature of interest in the present work is the transition occurring at about  $-55^{\circ}\text{C}$ . Since the material begins to soften at that temperature, the event is attributed to the glass transition. Further evidence is shown in Figure 2 where the DSC data are plotted. A feature typical of a glass transition is observed beginning at about  $-67^{\circ}$  and ending at about  $-47^{\circ}\text{C}$ . The central glass transition temperature,  $-57^{\circ}\text{C}$ , is about  $5^{\circ}$  lower than for the higher EO content siloxane polymer studied previously.<sup>5</sup> The center of the DSC glass transition occurs at approximately the same temperature as the low temperature TMA softening.

A second feature is observed in the DSC which was not observed previously.<sup>5</sup> Specifically, there is an event at about  $0^{\circ}\text{C}$ . A corresponding feature was not observed in the TMA studies. Heating the sample at about  $130^{\circ}\text{C}$  decreased the temperature of this feature to about  $-15^{\circ}\text{C}$ . Because of the variability of the temperature of this feature, it is not attributable to water. It is, in fact, similar to the DSC scans of Fish et al.<sup>3</sup> for a non-crosslinked ion containing siloxane polymer and thus the event may somehow be associated with the absence of crosslinking in regions of the material.

## Electrical Conductivity

A typical low temperature complex impedance plot is shown in Figure 3. The data were analyzed using a Cole-Cole distribution:<sup>6</sup>

$$Z^* = \frac{Z_0}{1 + (i\omega\tau_0)^{(1-\alpha)}} \quad (1)$$

where  $Z_0$ ,  $\tau_0$ , and  $\alpha$  are the fitting parameters. As temperature increases, less of a semicircle is observed together with more slanted vertical line at lower frequencies representing blocking electrode effects. In most cases, a best-fit of equation (1) to the data was obtained allowing values for the bulk resistance of the materials to be determined. For the remaining plots, a combination of the depressed arc and slanted vertical line was used to determine the bulk resistance.

The conductance values,  $G$ , were then used, in conjunction with room temperature geometrical measurements, to calculate the electrical conductivity from:

$$\sigma = Gt/S \quad (2)$$

where  $t$  is the thickness and  $S$  is the surface area. Thermal expansion effects are not included in the data analysis. The results of a typical vacuum data run are shown in Figure 4. The curvature often observed for amorphous polymer systems is apparent. Consequently, the conductivity data were first analyzed via the VTF equation:<sup>7</sup>

$$\sigma = AT^{-1/2} \exp^{-[E_a/k(T-T_0)]} \quad (3)$$

with the adjustable parameters A,  $E_a$ , and  $T_0$ . A non-linear least squares fit of equation (3) to the data was carried out and Table 1 contains the best-fit parameters.

It is noted that the vacuum values for  $T_0$  are about 40°C lower than the "central"  $T_g$ 's which were determined by DSC or the softening temperature as determined by TMA. This result is consistent with all previous work by the authors.<sup>5,8,9</sup> Such results are not unexpected since  $T_g - T_0$  is often on the order of 50°C for polymer systems.<sup>10,11</sup> Further, this phenomenon is consistent with the configurational entropy model<sup>12,13</sup> where  $T_0$  is interpreted as the temperature of zero configurational entropy which would be expected to occur at a much lower temperature than DSC  $T_g$ 's. However, this result disagrees with those of other workers<sup>12</sup> for similar materials. Possible reasons for the discrepancy along with details of the data analysis technique used in the present work are given elsewhere.<sup>5</sup>

Next, isothermal data were taken and typical results are shown in Figure 5. The following equation:

$$\log_{10} \sigma = \log_{10} \sigma_0 + aP + bP^2 \quad (4)$$

was best fit to the isothermal data and the best-fit parameters are listed in Table 2. The values listed in Table 2 for  $\log_{10} \sigma_0$  are those calculated from the vacuum data i.e. absolute conductivities were not determined for the pressure runs. Rather, relative changes were determined and the absolute value normalized to the more accurate vacuum data.

The isothermal studies can also be used to determine activation volumes directly via:

$$\Delta V^* = -kT \, d \ln \sigma / dP \quad (5)$$

The zero pressure values, those calculated from the slope of the conductivity vs. pressure plot at  $P=0$ , are listed in Table 2. The magnitude of the activation volumes is consistent with results for other ion conducting polymers and it is clear that they decrease as temperature increases. Also, the curvature of the  $\text{Log}(\sigma)$  versus pressure plot, which is related to the parameter  $b$  listed in Table 2, is negative at the lowest temperatures, becoming less so as temperature increases. Both results are similar to results for PPO complexed with lithium salts reported previously when the same analysis techniques were used<sup>8,9</sup> but opposite from the case of a single frequency analysis of results on ion containing PEO presented earlier.<sup>14</sup>

Next, the isothermal pressure data were used to generate 0.1 and 0.2  $\mu\text{Pa}$  conductivities. The results were best fit to equation (3) and the parameters are listed in Table 1. Both the data and best fit curves are plotted in Figure 4. It is found that  $T_0$  increases about 5 K/kbar. This is between the trends observed for  $\text{PPO}_8\text{LiCF}_3\text{SO}_3$  which showed a shift of about 10 K/kbar and  $\text{PPO}_8\text{LiClO}_4$  and  $\text{PPO}_8\text{LiI}$  for which the shift was very small. Since glass transitions usually shift several K/kbar, this result is consistent with the usual assertion that  $T_0$  is somehow associated with  $T_g$ . Obviously, the configurational entropy model provides such an interpretation.

Further, it is found that  $E_a$  also increases with pressure. As pointed out previously,<sup>9</sup> this provides evidence against "liquid-like" conductivity in these materials.

Next, the data were analyzed in terms of the WLF equation:<sup>11</sup>

$$\log_{10} \frac{\sigma(T)}{\sigma(T_g)} = \frac{C_1(T-T_g)}{C_2+(T-T_g)} \quad (5)$$

The resultant parameters are listed in Table 3. The values of  $C_1$  and/or  $C_2$  are somewhat lower than the "universal" values of 17.4 and 51.6.

Finally, for completeness, the data were analyzed via the mathematically equivalent VTF equation in the form:

$$\sigma = A' \exp^{-[E'_a/(T-T'_o)]} \quad (6)$$

The results are listed in Table 1. It is interesting that on the basis of the RMS deviation it is equation 3 which best fits the data.

#### Nuclear Magnetic Resonance

The  $^{23}\text{Na}$  absorption was previously shown to consist of a relatively narrow line with a short (approximately 1 ms) spin-lattice relaxation time ( $T_1$ ) superimposed on a long  $T_1$  (approximately 1 s) second-order quadrupole broadened line.<sup>5</sup> The composite NMR lineshape for the original sample,<sup>5</sup> hereafter denoted as sample A, is shown in Figure 6a. The dotted portion represents the absorption spectrum corresponding to the narrow line, which is obtained by saturating the long  $T_1$  component. The spectra were taken at  $-76^\circ\text{C}$ , well below  $T_g$ , with sequence delays of 10s and 40 ms for the

unsaturated and saturated lines, respectively. Figure 6b displays both unsaturated and partially saturated spectra (at  $T = -100^{\circ}\text{C}$ ) for the present lower EO-content complex, hereafter denoted as sample B. The primary difference between the two samples appears to be the greater degree of broadening in the broad component of A. In fact, the broad line of B (Figure 6b) is not second order quadrupole broadened as determined by the values of the  $\pi/2$  pulse widths for each lineshape component. The full-width at half-maximum (FWHM) of the narrow line of B remains relatively constant at approximately 5 kHz until about  $T_g$ , then narrows to a minimum of 1 kHz at about  $-5^{\circ}\text{C}$ . At higher temperature, the line gradually broadens to about 1.7 kHz as a result of extremely rapid spin-lattice relaxation. The FWHM of the broad line of B remains between 7 and 10 kHz over the temperature range  $-100$  to  $100^{\circ}\text{C}$ . However, a transition from first to second order quadrupole broadening occurs at about  $25^{\circ}\text{C}$ . This is in contrast to the results for sample A in which the broad component exhibits second order quadrupole effects over the entire temperature range.<sup>5</sup>

A common feature of samples A and B is the presence of both the broad and narrow lineshape components throughout the temperature range  $-100$  to  $100^{\circ}\text{C}$ . As the difference between the  $T_1$  values of the two components was always at least a factor of 100,<sup>5</sup> the individual contributions of each line to the composite lineshape and hence their relative intensities could be determined easily. The ratio of narrow to broad line intensity as a function of temperature (for sample B) is shown in Figure 7.

The short- $T_1$ , narrow line has been previously identified with highly mobile  $\text{Na}^+$  ions.<sup>5</sup> Among the possible configurations giving rise to the

long- $T_1$ , broad line are sodium ions rigidly bonded to the host polymer chains, and isolated cation-anion pairs or clusters. The presence of ion pairs in conducting polymer complexes has been inferred from a variety of measurements including vibrational spectroscopy<sup>10</sup> and pulsed field gradient NMR.<sup>15</sup> Conductivity measurements as a function of salt concentration in low molecular weight polyethers suggest that neutral ion pairs and charged ion triplets are the predominant salt species at low salt concentration.<sup>16</sup>

The possibility that the  $^{23}\text{Na}$  broad line might be associated with ion pairs or higher aggregates is given credence by known quadrupole coupling constants for  $\text{Na}^+$ -anion pairs in the gas phase.<sup>17</sup> Figure 7 may then be representative of a temperature dependent pair (or aggregate) dissociation process, although the presence of an alternative Na configuration for the broad line, such as bonded to the polymer chains, cannot be ruled out. It is interesting to note that, according to the data in Figure 7, the  $\text{Na}^+$  ion concentration increases by only a factor of 10 from  $-100$  to  $+100^\circ\text{C}$ , while the conductivity exhibits roughly a five order of magnitude increase over the same range. Thus, it appears that large scale segmental motion of the polymer chains implied by the VTF behaviour of the conductivity plays a much greater role than "carrier generation" in the transport process. A similar conclusion has been drawn by Watanabe et al.<sup>18</sup> who inferred the presence of a weakly temperature dependent dissociation process from time-of-flight mobility measurements in Li-PPO complexes.

Although there is considerable uncertainty in the higher temperature data of Figure 7 (due to the low signal to noise ratio characteristic of the broad line above room temperature) it is clear that the  $\text{Na}^+$  ion

concentration (narrow line) does not continue to increase with increasing temperature, at least not at the rate observed at lower temperatures. There is presently no satisfactory explanation for this observation, nor does the high temperature scatter of the data permit further speculation on this point. The final comment concerns the previously mentioned transition to second order quadrupole broadening above room temperature. For the NMR frequency employed (81 MHz), second order broadening implies a quadrupole coupling constant on the order of 1 MHz, which is comparable to that of a  $\text{Na}^+$ -anion pair.<sup>17</sup> It can be shown<sup>19</sup> that the quadrupole coupling associated with a sodium ion in contact with a neutral ion-pair i.e. an ion triplet, is somewhat smaller than for a sodium ion in contact with an anion, i.e. an ion pair. Thus, the presence of a significant number of triplets which are converted to single ions and ion pairs above room temperature could provide an explanation for the observed broadening. Further evidence for or against this simple model will require more accurate narrow/broad ratios as well as better estimates of quadrupole coupling constants from the observed lineshapes.

#### SUMMARY

In summary, then, the following results have been obtained.

(a) Vacuum electrical conductivity measurements have been performed and are analyzed in terms of VTF and WLF equations. The most important result is that for the VTF equation  $T_0$  is found to be about 45°C below the "central"  $T_g$ . This is consistent with the usual behavior of these quantities and is predicted by the configurational entropy model. As regards the WLF equation, the values of  $C_1$  and/or  $C_2$  are found to be slightly lower than the "universal" values.

(b) High pressure electrical conductivity measurements have also been performed and a VTF analysis shows that  $T_0$  increases about 50 K/GPa and  $E_a$  increases significantly. In addition, the activation volume associated with the electrical conductivity decreases as temperature increases as expected.

(c)  $^{23}\text{Na}$  NMR-determined mobile to bound sodium ratios exhibit a factor of 10 increase over the temperature range  $-100$  to  $+100^\circ\text{C}$ , in contrast with the  $10^5$  increase in the conductivity over the same range. Thus, carrier generation plays a relatively minor role in the transport mechanism.

#### ACKNOWLEDGMENTS

The authors acknowledge Mr. Yiu Sun Pak and Ms. Meng Chiao for assistance with the NMR measurements and data analysis. This research was supported in part by the Office of Naval Research and the PSC-CUNY Research Award Program.

#### REFERENCES

1. Nagaoka, K., Naruse, H., Shinohara, I., and Watanabe, M., J. Polym. Sci, Polym. Letters Edn. 1984, 22, 659
2. Bouridah, A., Dalard, F., Deroo, D., Cheradame, H., and Le Nest, J. F., Solid State Ionics 1985, 15, 233
3. Fish, D., Khan, I. M., and Smid, J., Makromol. Chem., Rapid Commun. 1986, 7, 115
4. Hall, P. G., Davies, G. R., McIntyre, J. E., Ward, I. M., Bannister, D. J., and Le Brocq, K. M. F. Polymer Comm., 1986, 27, 98
5. Adamic, K. J., Greenbaum, S. G., Wintersgill, M. C., and Fontanella, J. J., J. Appl. Phys. 1986, 60, 1342
6. Cole, K. S., and Cole, R. H., J. Chem. Phys. 1941, 9, 341
7. Vogel, H., Physik Z. 1921, 22, 645; Tammann, V. G., and Hesse, W., Z. Anorg. Allg. Chem. 1926, 156, 245; Fulcher, G. S., J. Am. Ceram. Soc. 1925, 8, 339
8. Fontanella, J. J., Wintersgill, M. C., Calame, J. P., Smith, M. K., and Andeen, C. G., Solid State Ionics (1986), 18&19, 253
9. Fontanella, J. J., Wintersgill, M. C., Smith, M. K., Semancik, J., and Andeen, C. G., J. Appl. Phys. 1986, to be published, October
10. Papke, B. L., Ratner, M. A., and Shriver, D. F., J. Electrochem. Soc. 1982, 129, 1694
11. Angell, C. A., Solid State Ionics 1983, 9&10, 3
12. Gibbs, J. H. and DiMarzio, E. A., J. Chem. Phys. 1958, 28, 373
13. Adam, G. and Gibbs, J. H., J. Chem. Phys. 1965, 43, 139
14. Fontanella, J. J., Wintersgill, M. C., Calame, J. P., Pursel, Figueroa, D. R., and Andeen, C. G., Solid State Ionics 1983, 9&10, 1139

15. Bhattacharja, S., Smoot, S. W., and Whitmore, D. H., Solid State Ionics 1986, 18&19, 306
16. Hall, P. G., Davies, G. R., Ward, I. M., and McIntyre, J. E., Polymer Comm. 1986, 27, 100
17. Semin, G. K., Barbushkina, T. A., and Yakobson, G. G., 'Nuclear Quadrupole Resonance in Chemistry,' John Wiley and Sons, New York, 1975.
18. Watanabe, M., Sanui, K., Ogata, N., Kobayashi, T., and Ohtaki, Z., J. Appl. Phys. 1985, 57, 123
19. Cohen, M. H. and Reif, F., 'Solid State Physics,' edited by Seitz, F. and Turnbull, D., Academic Press, New York, 1957.

Table 1. Best fit VTF parameters.

	RMS Deviation	$\log_{10} A$ $(\Omega\text{-cm})^{-1}$	$E_a$ (eV) - $\sqrt{K}$	$T_o$ (K)	RMS Deviation	$\log_{10} A'$ $(\Omega\text{-cm})^{-1}$	$E'_a$ (eV)	$T'_o$ (K)
Vacuum	0.0120	-0.63	0.102	171.7	0.0130	-2.03	0.097	173.5
0.1 GPa	0.0051	-0.43	0.115	176.7	0.0052	-1.81	0.111	178.1
0.2 GPa	0.0102	-0.26	0.127	181.3	0.0104	-1.63	0.123	182.4

Table 2. Best fit parameters in equation 4 and activation volumes for isothermal data.

Maximum pressure (GPa)	T(K)	RMS Deviation	$\log_{10} \sigma_0$ $(\Omega\text{-cm})^{-1}$	$a(\text{GPa})^{-1}$	$b(\text{GPa})^{-2}$	$\Delta V^*$ $(\text{cm}^3/\text{mol})$
0.15	262.2	0.0031	-7.530	-8.77	-2.21	44.0
0.27	266.5	0.0034	-7.276	-8.19	-1.44	41.8
0.23	272.3	0.0045	-6.968	-7.51	-1.48	39.1
0.30	280.5	0.0078	-6.588	-6.54	-0.70	35.1
0.60	306.6	0.0190	-5.692	-4.44	-0.49	26.1
0.55	317.9	0.0098	-5.405	-3.91	-0.23	23.8
0.40	323.4	0.0073	-5.281	-3.75	+0.17	23.2

Table 3. DSC results and best fit WLF parameters.

	$T_g$ (K)	$C_1$	$C_2$ (K)	$\log_{10} \sigma(T_g) (\Omega\text{-cm})^{-1}$	RMS Deviation
Onset	206	15.0	32.5	-17.0	0.0130
Central	216	11.5	42.5	-13.5	0.0130
End	226	9.3	52.5	-11.3	0.0130

#### FIGURE CAPTIONS

Figure 1. TMA plot showing the glass transition at about  $-55^{\circ}\text{C}$ . The data were taken at 5 K/min.

Figure 2. DSC plot showing the glass transition at about  $-55^{\circ}\text{C}$ . The data were taken at 10 K/min.

Figure 3. Complex impedance plot at 254K. + shows the center of the depressed Cole-Cole arc and x represents the bulk resistance of the sample. The squares represent the datum points and the solid line is the best fit Cole-Cole equation (equation 1).

Figure 4. Arrhenius plot of the electrical conductivity data. From top to bottom the data are vacuum (triangles), 0.1 GPa (diamonds), and 0.2 GPa (stars). The solid lines are the best fit VTF equation (equation 3).

Figure 5. Typical data and best-fit quadratic (equation 4) for the pressure dependence of the electrical conductivity. The data are at 306.6 K.

Figure 6.  $^{23}\text{Na}$  NMR absorption spectra for (a) sample A, and (b) sample B (lower EO-content than A). The dotted curves in (a) and (b) are spectra obtained with a short sequence delay, in which the broad components are completely saturated.

Figure 7. Reciprocal temperature plot of narrow to broad line intensity ratios for sample B.

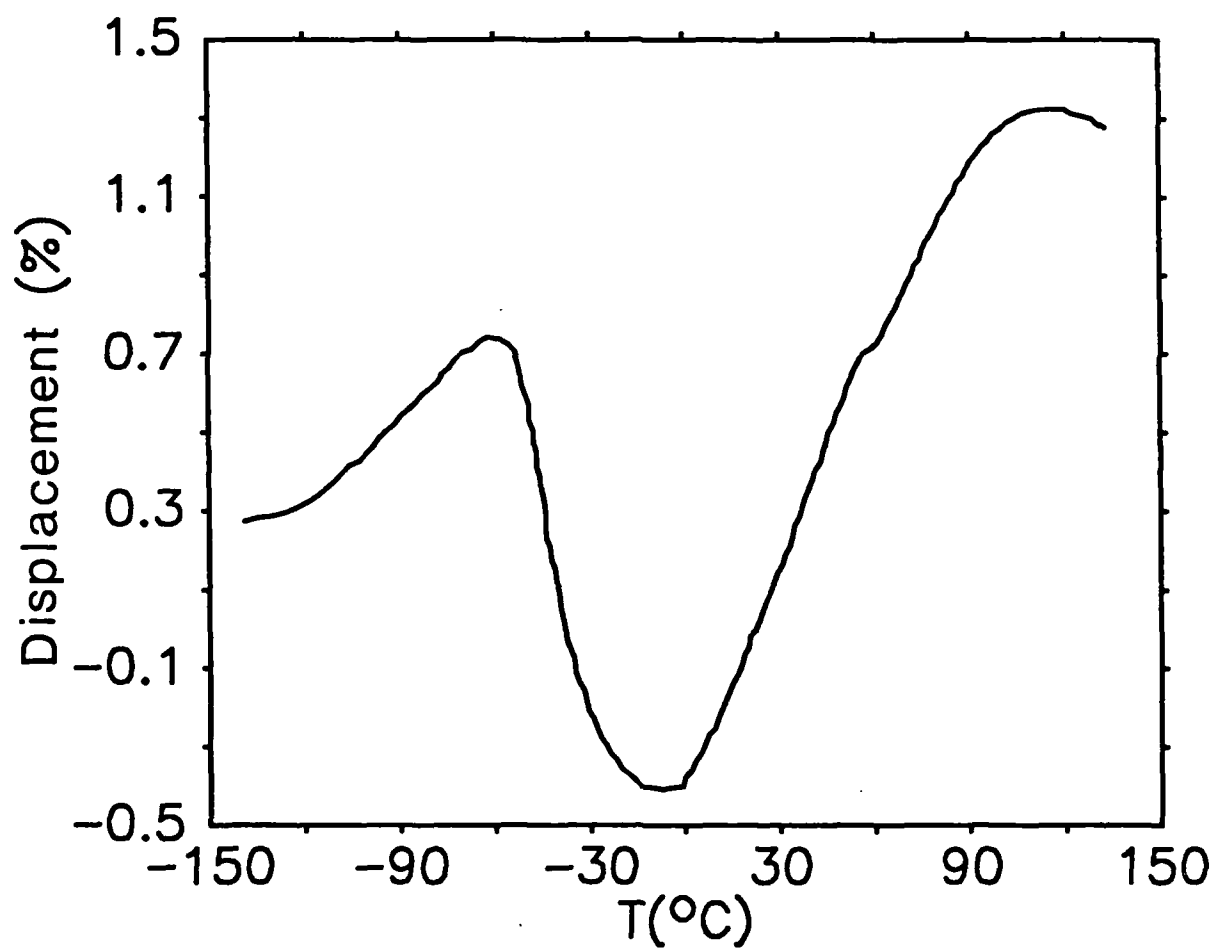


Fig. 1 Wintersgill et al.

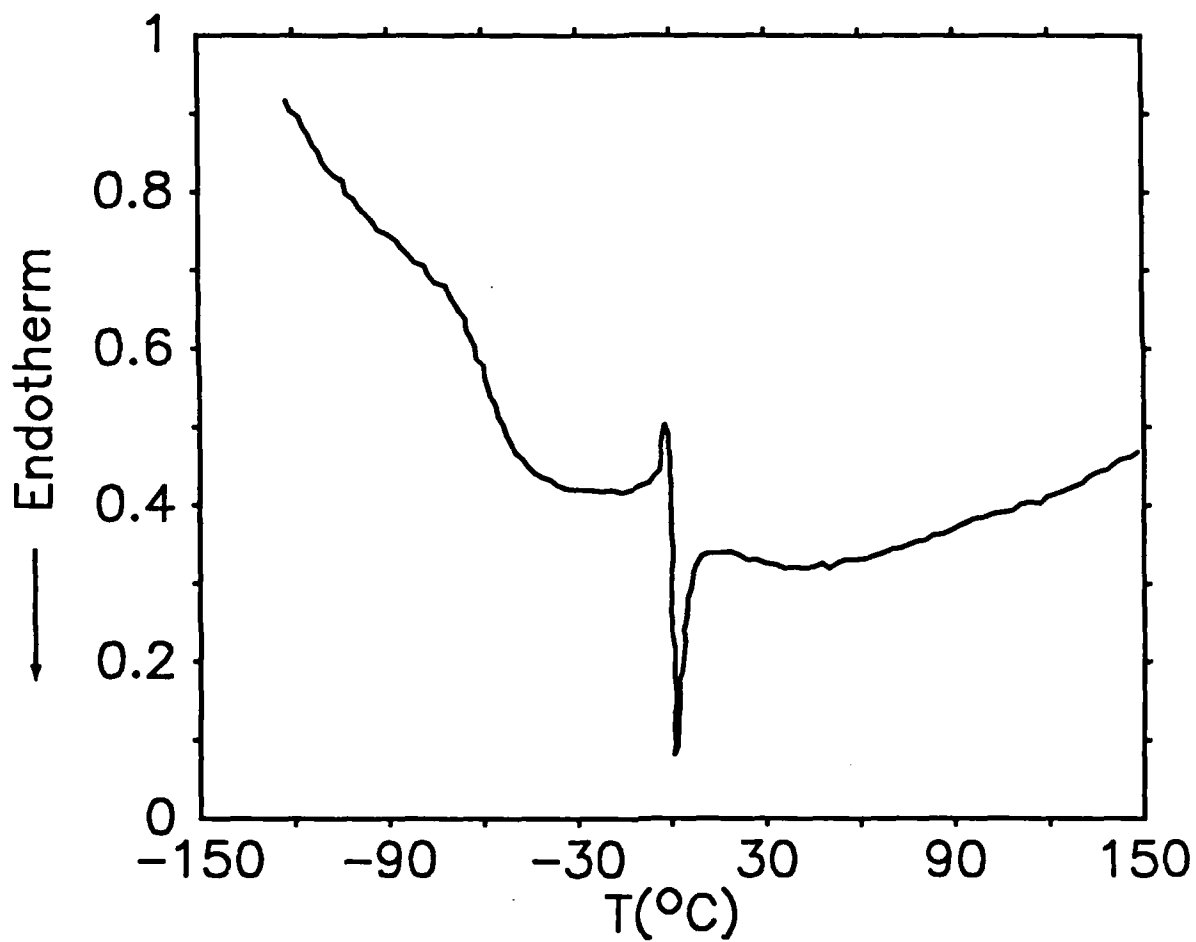


Fig 2 Wintergill et al.

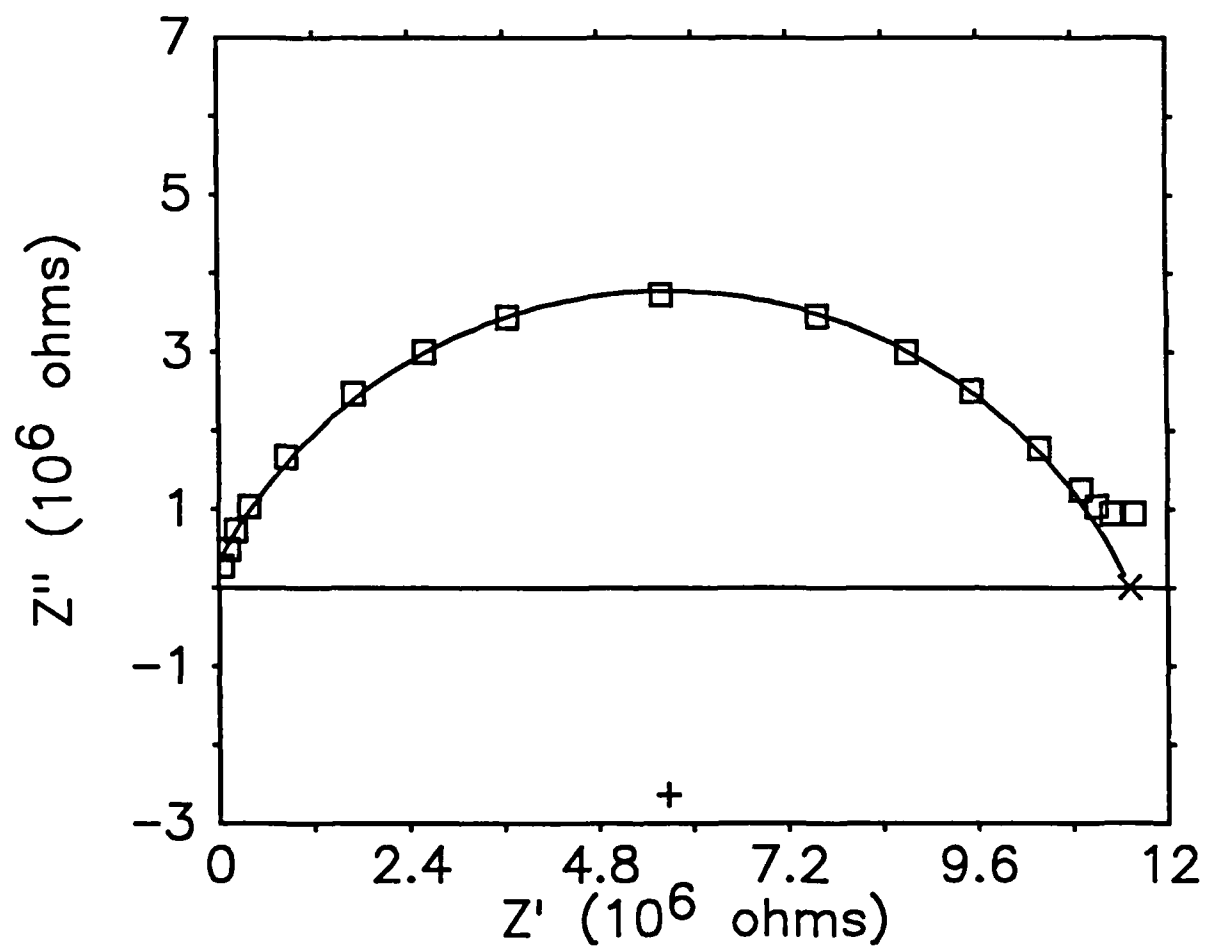


Fig. 3 W. J. ... et al

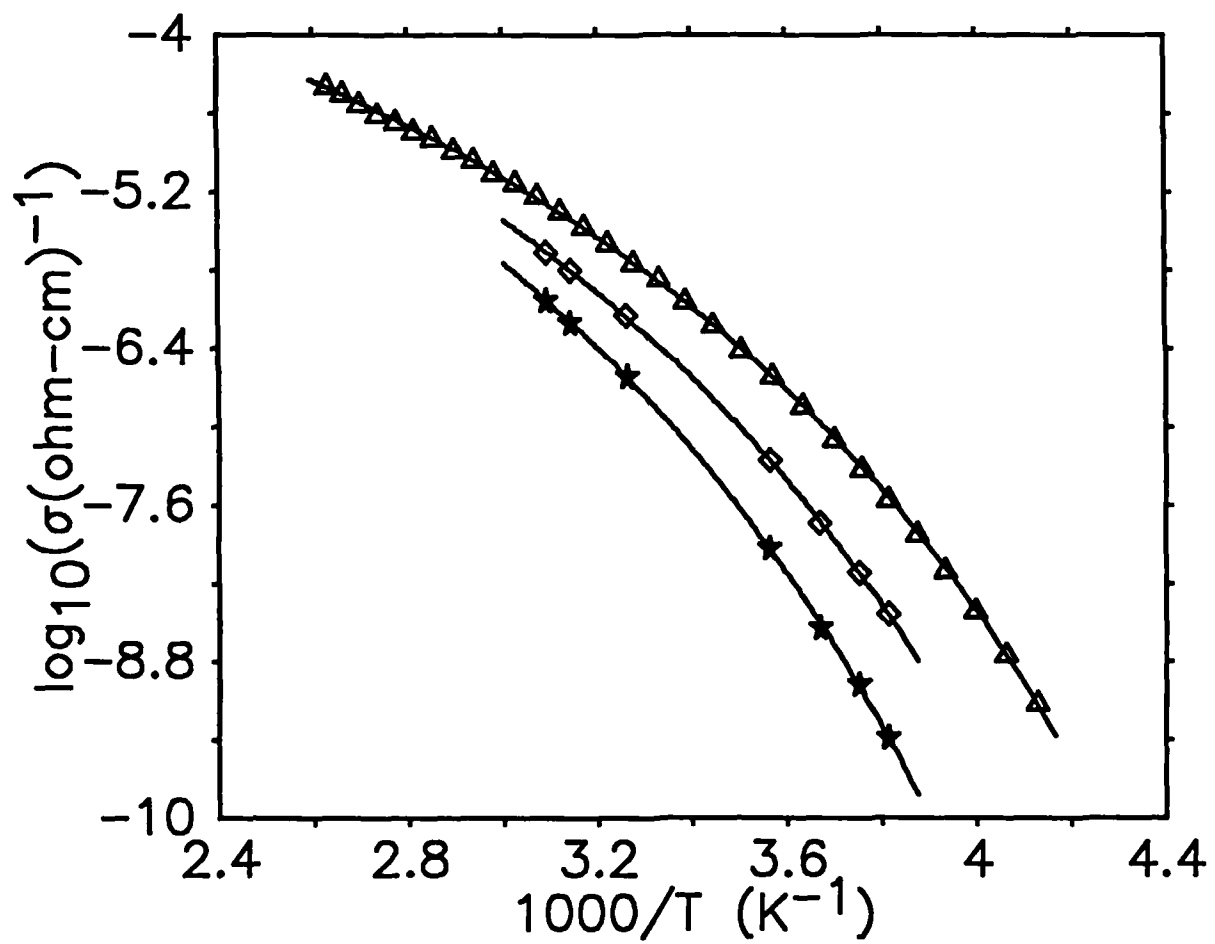


Fig. 4 Wintersgill et al.

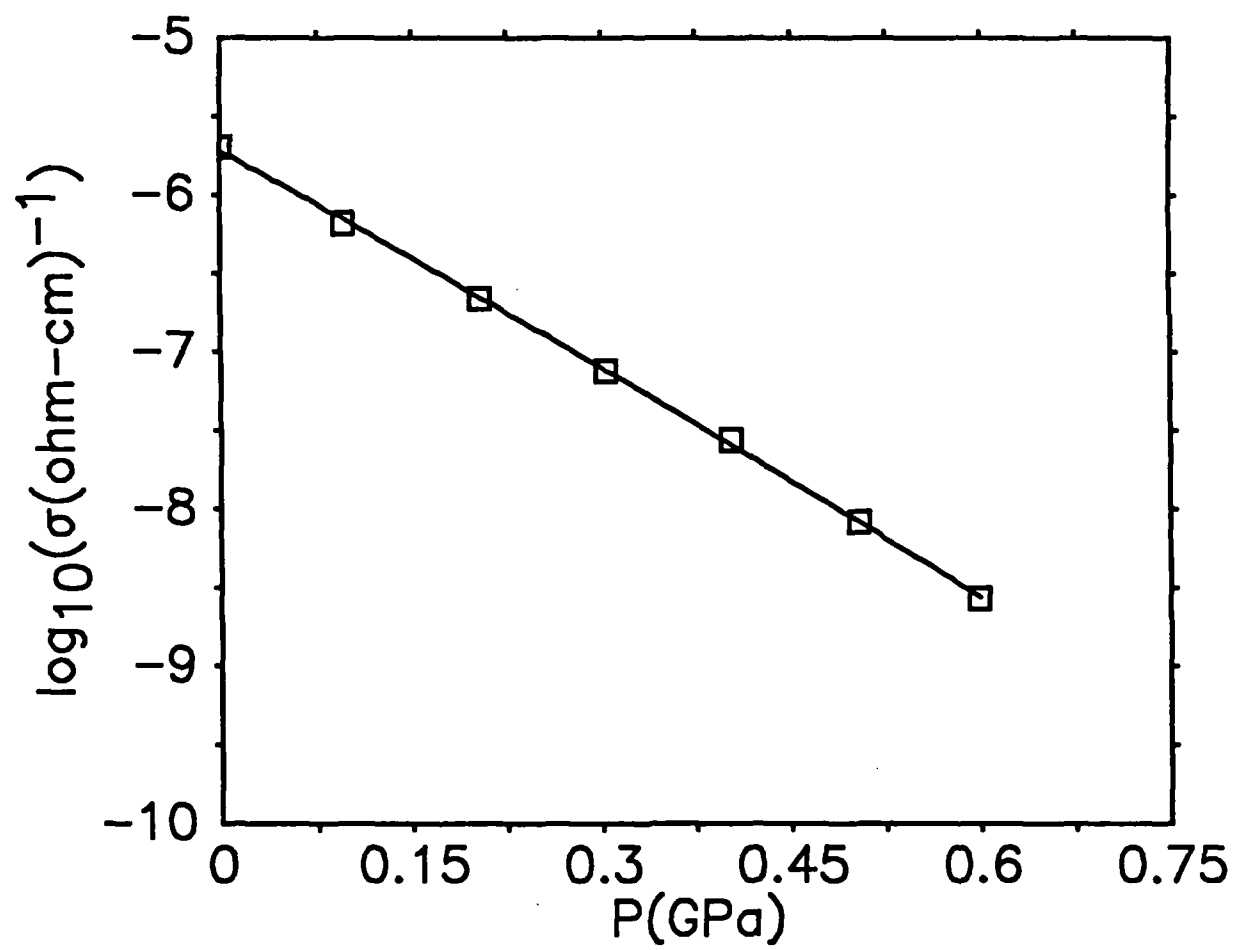
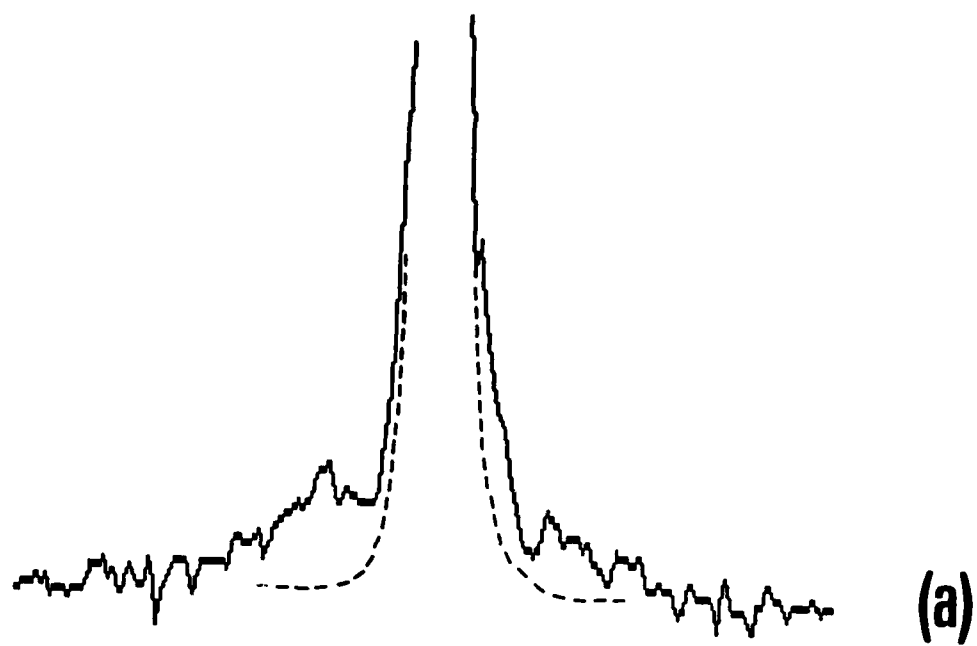


Fig. 5 Wintersill et al.



20 kHz

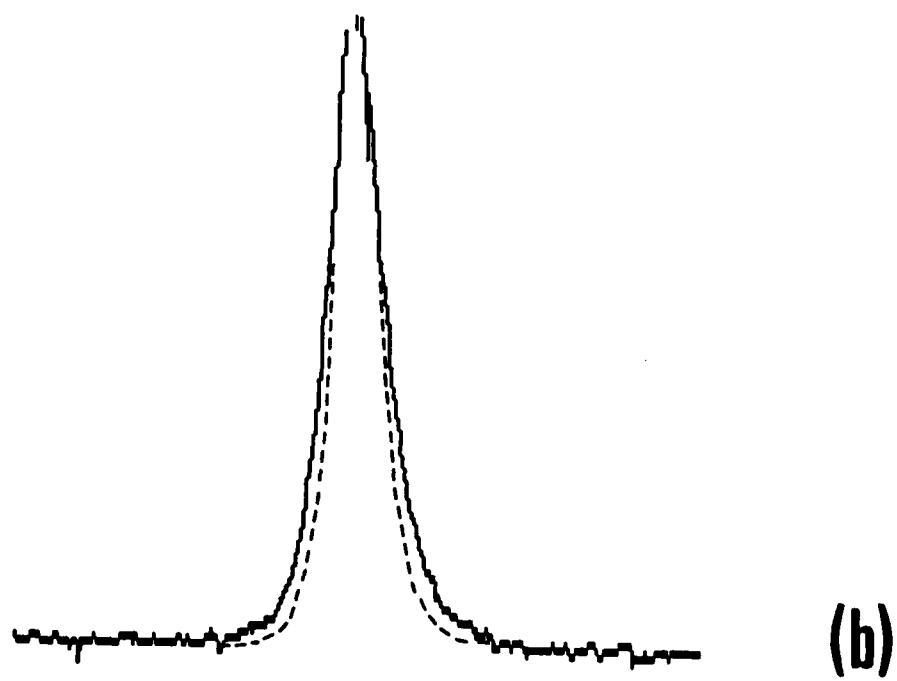


Fig. 6

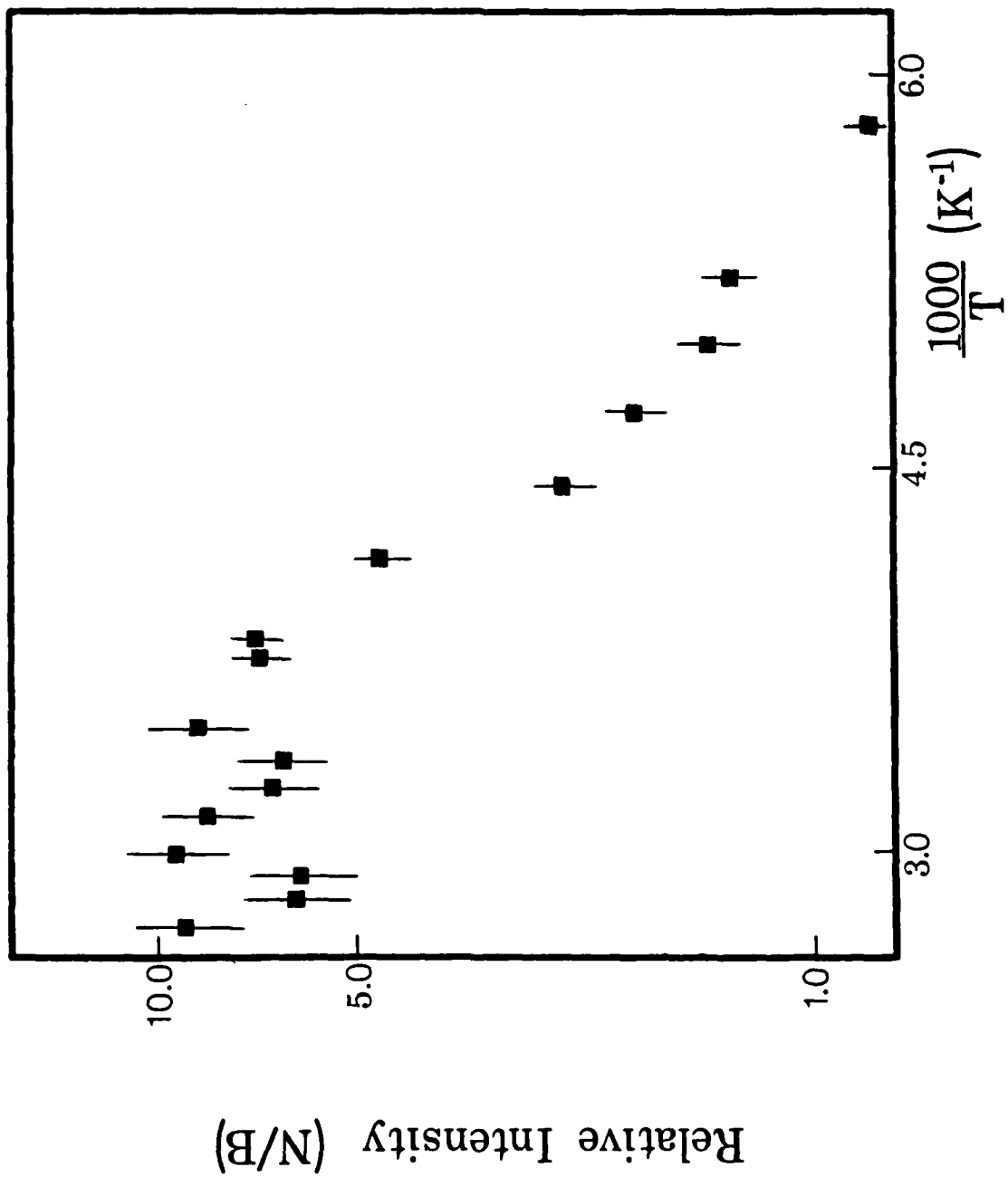


Fig. 7

TECHNICAL REPORT DISTRIBUTION LIST, GEN

	<u>No. Copies</u>		<u>No. Copies</u>
Office of Naval Research Attn: Code 1113 800 N. Quincy Street Arlington, Virginia 2217-5000	2	Dr. David Young Code 334 NORDA NSTL, Mississippi 39529	1
Dr. Bernard Douda Naval Weapons Support Center Code 50C Crane, Indiana 47522-5050	1	Naval Weapons Center Attn: Dr. Ron Atkins Chemistry Division China Lake, California 93555	1
Naval Civil Engineering Laboratory Attn: Dr. R. W. Drisko, Code L52 Port Hueneme, California 93401	1	Scientific Advisor Commandant of the Marine Corps Code RD-1 Washington, D.C. 20380	1
Defense Technical Information Center Building 5, Cameron Station Alexandria, Virginia 22314	12 high quality	U.S. Army Research Office Attn: CRD-AA-IP P.O. Box 12211 Research Triangle Park, NC 27709	1
DTNSRDC Attn: Dr. H. Singerman Applied Chemistry Division Annapolis, Maryland 21401	1	Mr. John Boyle Materials Branch Naval Ship Engineering Center Philadelphia, Pennsylvania 19112	1
Dr. William Tolles Superintendent Chemistry Division, Code 6100 Naval Research Laboratory Washington, D.C. 20375-5000	1	Naval Ocean Systems Center Attn: Dr. S. Yamamoto Marine Sciences Division San Diego, California 91232	1

END

10-86

DTIC